Original Article

Competitive antagonists facilitate the recovery from desensitization of α1β2γ2 GABA$_A$ receptors expressed in *Xenopus* oocytes

Xiao-jun XU[1, 2], Diane ROBERTS[2], Guo-nian ZHU[1], Yong-chang CHANG[2, *]

[1]*Institute of Pesticide and Environmental Toxicology, Zhejiang University, Hangzhou 310029, China;* [2]*Division of Neurobiology, Barrow Neurological Institute, St Joseph's Hospital and Medical Center, Phoenix, AZ 85013, USA*

Aim: The continuous presence of an agonist drives its receptor into a refractory state, termed desensitization. In this study, we tested the hypothesis that a competitive antagonist, SR95531, could facilitate the recovery of α1β2γ2 GABA$_A$ receptor from functional desensitization.

Methods: α1β2γ2 GABA$_A$ receptors were expressed in *Xenopus* oocytes. GABA-evoked currents were recorded using two-electrode voltage-clamp technique. Drugs were applied through perfusion.

Results: Long application of GABA (100 µmol/L) evoked a large peak current followed by a small amplitude steady-state current (desensitization). Co-application of SR95531 during the desensitization caused a larger rebound of GABA current after removal of SR95531. Furthermore, application of SR95531 after removal of GABA increased the rate of receptor recovery from desensitization, and the recovery time constant was decreased from 59±3.2 s to 33±1.6 s. SR95531-facilitated receptor recovery from desensitization was dependent on the perfusion duration of SR95531. It was also dependent on the concentration of SR95531, and the curve fitting with Hill equation revealed two potency components, which were similar to the two potency components in inhibition of the steady-state current by SR95531. Bicuculline caused similar facilitation of desensitization recovery.

Conclusion: SR95531 facilitates α1β2γ2 GABA$_A$ receptor recovery from desensitization, possibly through two mechanisms: binding to the desensitized receptor and converting it to the non-desensitized state, and binding to the resting state receptor and preventing re-desensitization.

Keywords: GABA$_A$ receptor; desensitization; GABA; SR95531; bicuculline; *Xenopus* oocytes

Introduction

The pentameric ligand-gated ion channel superfamily has been traditionally named the cys-loop receptor family of ligand-gated ion channels[1, 2]. This family includes vertebrate nicotinic acetylcholine receptors[3], serotonin type 3 receptors[4], GABA$_{A/C}$ receptors[5], glycine receptors[6], the zinc-activated cation channel[7], invertebrate glutamate-gated chloride channels[8], GABA-gated cation channels[9], histamine-[10] or serotonin-[11] gated chloride channels, and bacterial channels such as the *Gloeobacter violaceus* ligand-gated ion channel (GLIC) and the *Erwinia chrysanthemi* ligand-gated ion channel (ELIC)[12, 13]. The binding of a neurotransmitter to the binding site of its receptor activates the receptor to open an inte-

gral channel[14–16]. However, the binding of the agonist to its receptor also drives the receptor into a refractory state, called desensitization[17]. The rate and extent of desensitization vary significantly among different receptor types and subtypes, depending on their subunit composition[18]. Variation in desensitization helps to shape synaptic transmission[19] for different needs.

The cys-loop receptors are allosteric proteins in which the extracellularly located neurotransmitter binding site is coupled to the transmembrane channel gate through an interconnected allosteric network[20, 21]. Ligand binding and channel gating can mutually influence each other[15, 22]. Agonist binding can drive the receptor from the resting state to the open state and the desensitization state and involves conformational changes not only in the channel gate but also in the binding site[23]. Thus, the affinity of a receptor to agonists or to antagonists depends on the state of the receptor. An agonist-

induced high-affinity desensitized state was proposed more than half a century ago[17]. However, even with high affinity, agonists can dissociate from a desensitized receptor at faster rates than a receptor can recover from desensitization. This is the basis for the cyclic model, in which the receptor can recover to the resting state directly from the desensitized state. The original cyclic model resulted from the study of the nicotinic receptor and is supported by studies of GABA receptors[24, 25], as well as studies of other members of this receptor family[26]. We previously showed that radio-labeled GABA binding can only be used to measure $\alpha 1\beta 2\gamma 2$ GABA$_A$ receptor binding in the desensitized state because of the high affinity (K_d=40 nmol/L) of the receptor and slow dissociation of the agonist[24]. Although open receptor states have relatively high affinity, their sub-second fast deactivation kinetics, even at a low temperature, make it impossible to separate bound ligand from free ligand when measuring radio-ligand binding. The affinities of the resting state and the open state of a typical GABA$_A$ receptor to GABA were determined by fitting the concentration-dependent activations of the wild type and channel-gate loosening mutants at the 9' position ($\alpha 1$L263S, $\beta 2$L259S, $\gamma 2$L274S) to the Monod-Wyman-Changeux (MWC) allosteric model with a resting state K_d of 78.5 μmol/L and an open state K_d of 120 nmol/L[27]. Thus, the affinity of a ligand-gated ion channel for its agonist is state dependent, with low affinity in the resting closed state, higher affinity in the open state, and the highest affinity in the desensitized state.

A competitive antagonist binds to the orthosteric binding site of the receptor and thereby directly competes with the agonist for the same binding site. Although it may appear that a competitive antagonist simply blocks the binding of the agonist without its own intrinsic activity on the receptor, many competitive antagonists are actually inverse agonists[15]. Studies have shown that SR95531 (gabazine) and bicuculline, which are competitive antagonists for the GABA$_A$ receptor, not only compete with GABA for binding but also have a negative impact on the channel gating that is induced by allosteric activators (such as neurosteroids and barbiturates[28]) and on the spontaneously opening mutant GABA$_A$ receptors[27]. It has been proposed that SR95531 and bicuculline can act as inverse agonists at the GABA binding site, similar to the action of a benzodiazepine inverse agonist at the benzodiazepine binding site[29]. However, experimental evidence for whether these competitive antagonists have an opposing effect on GABA-induced desensitization is lacking. Based on their antagonistic effect on channel opening, we hypothesized that SR95531 and bicuculline could antagonize GABA-induced desensitization. Specifically, our hypothesis is that these competitive antagonists could facilitate receptor recovery from desensitization and prevent reentry of the receptor into the desensitized state after recovery. Because the $\alpha 1\beta 2\gamma 2$ GABA$_A$ receptor is the major subtype of GABA$_A$ receptors in the brain, we tested our hypothesis using two-electrode voltage-clamp studies of *Xenopus* oocytes that expressed this subtype of the GABA$_A$ receptor.

Materials and methods

cRNA preparation

The cDNA encoding the rat wild type $\alpha 1$, $\beta 2$, $\gamma 2$S GABA receptor subunits were cloned into the pGEM-T vector with T7 orientation to avoid overexpression-related changes in current kinetics in most experiments. These GABA-receptor subunit cDNAs were also cloned into the pGEMHE vector for overexpression in one experiment. The cDNA of the human $\rho 1$ GABA receptor subunit in pAlter-1, used in the supplementary data, was kindly provided by Dr David WEISS. The cDNAs for $\alpha 1$, $\beta 2$, and $\gamma 2$S were amplified by PCR with Phusion DNA polymerase (New England Biolabs, Ipswich, MA, USA) and M13 forward and reverse primers and were used as the DNA templates for cRNA synthesis. The cDNA of the human $\rho 1$ GABA receptor subunit was linearized by *Nhe* I and purified for cRNA synthesis. The cRNAs were transcribed by standard *in vitro* transcription using T7 RNA polymerase. After degradation of the DNA template by RNase-free DNase I, the cRNAs were purified and resuspended in diethyl pyrocarbonate (DEPC)-treated water. cRNA yield and integrity were examined with an Eppendorf BioPhotometer and a 1% agarose gel.

Oocyte preparation and injection

Oocytes were harvested from female *Xenopus laevis* (Xenopus I, Ann Arbor, MI, USA), using the protocol "Xenopus Care and Use" approved by the Institutional Animal Care and Use Committee of the St Joseph's Hospital and Medical Center. Briefly, the frogs were anesthetized with 0.2% MS-222 (tricaine methanesulfonate). The ovarian lobes were surgically removed and placed in an incubation solution consisting of (in mmol/L) 82.5 NaCl, 2.5 KCl, 1 MgCl$_2$, 1 CaCl$_2$, 1 Na$_2$HPO$_4$, 0.6 theophylline, 2.5 sodium pyruvate, and 5 HEPES; the incubation solution also contained 50 U/mL of penicillin and 50 μg/mL of streptomycin and had a pH of 7.5. After surgery, the frogs were given an analgesic, xylazine hydrochloride (10 mg/kg, intraperitoneal), and an antibiotic, gentamicin (3 mg/kg, intraperitoneal), and were allowed to recover from surgery before being returned to the incubation tank. The frogs were euthanized under anesthesia with MS-222 after the third surgery. The ovarian lobes were cut into small pieces and digested with 1.0 Wunsch unit/mL of Liberase Blendzyme™ (Roche Applied Science, Indianapolis, IN, USA), with constant stirring at room temperature for 1.5 to 2 h. The dispersed oocytes were thoroughly rinsed with the above solution. The stage VI oocytes were selected and incubated at 16 °C before injection. Micropipettes for injection were pulled from borosilicate glass on a Sutter P87 horizontal puller, and the tips were cut with forceps to approximately 40 μm in diameter. The cRNA was drawn up into the micropipette and injected into oocytes with a Nanoject Micro-injection System (Drummond, Broomall, PA, USA) at a total volume of approximately 20 to 60 nL.

Two-electrode voltage-clamp technique

Two to four d after injection, the oocytes expressing the wild-

type GABA$_A$ receptors were placed in a custom-made small volume chamber with continuous perfusion with oocyte Ringer's solution (OR2), which consisted of (in mmol/L) 92.5 NaCl, 2.5 KCl, 1 CaCl$_2$, 1 MgCl$_2$, and 5 HEPES, at pH 7.5. The chamber was grounded through an agar KCl bridge to prevent any ligand-induced junction potential change. The oocytes were voltage-clamped at -70 mV to measure GABA-induced currents using an AxoClamp 900A amplifier (Molecular Devices, Sunnyvale, CA, USA). The current signal was filtered at 50 Hz with the built-in 4-pole low-pass Bessel filter in the AxoClamp 900A and digitized at 100 Hz with the Digidata1440A digitizer (Molecular Devices) and pClamp10.

Drug preparation

Stock solutions of GABA, (–)-bicuculline methochloride, picrotoxin, zinc chloride, 3-aminopropylphosphonic acid (3-APA) (Sigma-Aldrich, St Louis, MO, USA), and SR95531 hydrobromide (Tocris, Bristol, UK) were prepared from the solids and stored at -20 °C in aliquots. Working concentrations of these drugs were prepared from the stock solutions immediately before use.

Kinetic simulations

For a better understanding of our experimental observations, we performed kinetic simulation using the QUB express software[30]. The software was downloaded from the web site http://www.qub.buffalo.edu/ and installed on a Dell Precision T5500 desktop computer. We used two kinetic models for the simulation. Comparison of the outputs from the two different models gave us new insights for data interpretation.

Scheme I is a linear model. It includes two binding steps for the agonist GABA (G) or two binding steps for the antagonist SR95531 (S) to bind the receptor (R). The GABA-bound receptor then undergoes transitions into the open state (O) and then into the desensitized state (D).
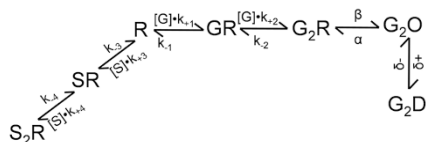
Scheme I.

Scheme II is a cyclic model that allows GABA to dissociate from the D-state, creating the opportunity for SR95531 binding
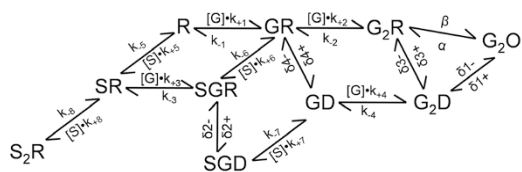
Scheme II.

to the D-state with a low affinity, and then SR95531 binding to the D-state facilitates desensitization recovery (with a very high ratio of δ2$^-$/δ2$^+$). To simplify the simulation, we only included a single step of GABA molecule dissociation from the D state. The numerical values of the rate constants used in the simulation are listed in Table 1.

Table 1. Rate constants used in simulations with the linear and cyclic models.

Linear model (Scheme I)		Cyclic model (Scheme II)	
k_{+1} (µmol·L^{-1}·s^{-1})	4	k_{+1} (µmol·L^{-1}·s^{-1})	4
k_{+2} (µmol·L^{-1}·s^{-1})	2	k_{+2} (µmol·L^{-1}·s^{-1})	2
k_{+3} (µmol·L^{-1}·s^{-1})	80	k_{+3} (µmol·L^{-1}·s^{-1})	1
k_{+4} (µmol·L^{-1}·s^{-1})	40	k_{+4} (µmol·L^{-1}·s^{-1})	32
k_1 (s^{-1})	130	k_{+5} (µmol·L^{-1}·s^{-1})	80
k_2 (s^{-1})	260	k_{+6} (µmol·L^{-1}·s^{-1})	40
k_3 (s^{-1})	10	k_{+7} (µmol·L^{-1}·s^{-1})	8
k_4 (s^{-1})	20	k_{+8} (µmol·L^{-1}·s^{-1})	40
α (s^{-1})	510	k_1 (s^{-1})	130
β (s^{-1})	2100	k_2 (s^{-1})	260
δ$^+$ (s^{-1})	30	k_3 (s^{-1})	130
δ$^-$ (s^{-1})	2	k_4 (s^{-1})	10
		k_5 (s^{-1})	10
		k_6 (s^{-1})	10
		k_7 (s^{-1})	200
		k_8 (s^{-1})	20
		α (s^{-1})	510
		β (s^{-1})	2100
		δ1$^+$ (s^{-1})	30
		δ1$^-$ (s^{-1})	2
		δ2$^+$ (s^{-1})	1
		δ2$^-$ (s^{-1})	1000
		δ3$^+$ (s^{-1})	2
		δ3$^-$ (s^{-1})	0.1
		δ4$^+$ (s^{-1})	1
		δ4$^-$ (s^{-1})	3

Note: The rate constants for channel activation were based on Amin and Weiss[31]. The desensitization and recovery rate constants were adjusted with a ratio of 15 to give a steady-state activation of 6.25% of its maximum open probability in the linear model. The values for the rate constants of desensitization and recovery are expected to be higher than those for the real GABA$_A$ receptor to give a shorter simulation time period. The rate constants for SR95531 high affinity binding were adjusted to give 260-fold higher affinity than that for GABA in the resting state, since the estimated K_i value for SR95531 is about 265-fold higher than the estimated GABA affinity in the resting state. The low affinity binding of SR95531 in the desensitized state was based on the experimental observation of a low sensitivity component, and its rate constants were estimated. High value of the ratio of δ2$^-$/δ2$^+$ was based on the assumption that SR95531 binding facilitates recovery of the receptor from desensitization.

Statistical analysis

The peak and steady-state currents of GABA-induced current were measured using Clampfit10.3. The current was measured relative to the baseline before GABA application. The

www.chinaphar.com
Xu XJ *et al*
1023

concentration-response relations of the current recovery facilitated by the antagonist or of the current inhibited by the antagonist were fit by a least-squares method to a Hill equation with GraphPad Prism 6.0 (GraphPad Software, Inc, La Jolla, CA, USA) to derive the EC_{50} or the IC_{50} (*ie*, the effective concentration or the inhibitory concentration, respectively, required for inducing a half maximal change) and the maximum current (I_{max}). The I_{max} was then used to normalize the concentration-response curves from individual oocytes. The average of the normalized currents or the changes for each agonist concentration were used to plot the data. The time course of desensitization recovery was fit by a least-squares method to a single exponential function to derive the time constant of recovery (τ). All data are presented as the mean±SEM (standard error of the mean). Statistical comparisons for $logEC_{50}$s, $logIC_{50}$s, or time constants were performed using two-sided grouped or paired (if two measurements were performed in the same oocytes) *t*-tests for two-group comparisons.

Results

SR95531-facilitated recovery from desensitization of the α1β2γ2 GABA receptor

Based on its ability to allosterically antagonize the neurosteroid activation of the $GABA_A$ receptor[28] and to antagonize the spontaneously opening of a mutant $GABA_A$ receptor[27], we hypothesized that SR95531 can antagonize GABA-induced desensitization and facilitate the recovery of the receptor from desensitization. To test this hypothesis, we applied a relatively high concentration of SR95531 to the $GABA_A$ receptor after it had reached steady state desensitization induced by adding 100 μmol/L GABA. Figure 1 shows that after adding 100 μmol/L GABA, the GABA-induced current had reached steady state and that subsequent co-application of 100 μmol/L SR95531 with 100 μmol/L GABA for 160 s clearly increased the recovery of the receptor from desensitization. The increased recovery is indicated by the several-fold higher current induced by the same GABA concentration upon removal of SR95531. Despite the continuous presence of a high concentration of GABA, SR95531 competition with GABA for binding in the steady state clearly re-sensitized the GABA receptor.

SR95531-facilitated recovery of desensitization is time dependent

A competitive antagonist can bind to the receptor only after dissociation of the agonist. Because a desensitized receptor has a much higher affinity for its agonist, the dissociation of GABA from the desensitized $GABA_A$ receptor is relatively slow. Thus, it can take some time for a competitive antagonist to bind to a significant number of receptors when the receptors are pre-occupied by the agonist. Figure 2 shows that the effect of SR95531 on the receptor recovery from desensitization in the presence of GABA was time dependent. The longer duration of the SR95531 application resulted in a higher recovery of the receptor from desensitization. The data are well fitted with a single exponential function with a relatively large time constant (194±21 s).
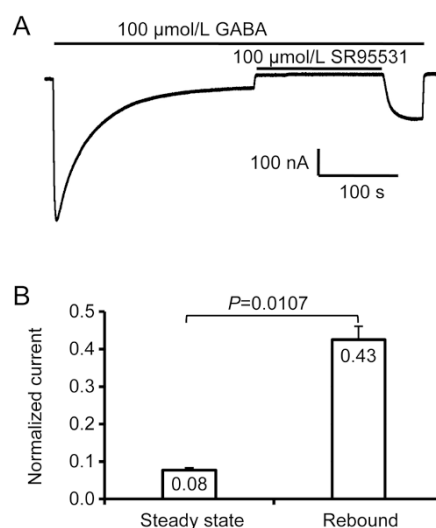

Figure 1. SR95531-facilitated recovery from desensitization of the α1β2γ2 GABA receptor. (A) Co-application of SR95531 and GABA after the GABA-induced current had reached steady state (with desensitization) caused current rebound after removing SR95531. (B) The rebound current normalized by the initial peak current and compared to the normalized steady-state current (*n*=6).
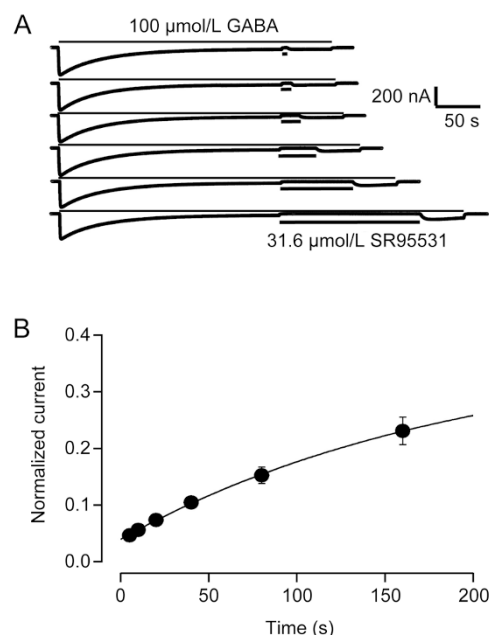

Figure 2. SR95531-facilitated recovery of desensitization (in the presence of GABA) is time dependent. (A) Raw current traces of the GABA-induced current with co-application of SR95531 and GABA with varied durations of SR95531 application. (B) Normalized (to the initial peak) recovery of GABA-induced current after SR95531 application (*n*=6).

SR95531-facilitated recovery of desensitization in the absence of GABA

If SR95531 could facilitate $GABA_A$ receptor recovery from

desensitization, we expected that it could also facilitate current recovery after removal of GABA. Figure 3 shows that upon termination of GABA application, application of SR95531 (followed by a 2-s OR2 application to allow SR95531 dissociation to reduce its antagonism) increased the recovery rate of the GABA response when compared to the recovery rate in the OR2 control. However, the recovery in SR95531 plateaued to approximately 71%±5% of its original peak value, likely due to incomplete dissociation of SR95531 during the subsequent 2-s OR2 application. In fact, our simulation result (Supplementary Figure S1) shows that the amplitude of rebound current is inversely related to the dissociation rate constant for SR95531. To experimentally confirm that incomplete recovery was mainly due to slow dissociation of SR95531, we set a control with only a brief initial GABA application for peak current measurement, waited for 180 s in OR2 for recovery of any desensitized receptors, and then pretreated the receptor with SR95531 followed by a 2-s OR2 application. Indeed, the SR95531 pretreatment alone (without desensitization) resulted in a lower amplitude of the second GABA response (Figure 3B, last trace). In fact, the response to the second GABA application after SR95531 pretreatment only reached 73%±4% of

the initial peak current. Using this control recovery fraction to normalize the desensitization recovery in the presence of SR95531, the percentage of desensitization recovery in the presence of SR95531 was similar to that in OR2 at 160 s. Interestingly, the recovery rate in the presence of SR95531 (τ=33±1.6 s) was faster than that in the OR2 control (τ=59±3.2 s).

SR95531-facilitated recovery of desensitization is concentration dependent

As a competitive antagonist, SR95531 would compete with GABA for the same available binding site after GABA dissociated from the receptor. Thus, for a fixed concentration of GABA, we expected to see a concentration-dependent effect of SR95531. Figure 4 shows that with greater concentrations of SR95531, the rebound current became higher. The increase in current recovery was not saturated at a 100 μmol/L concentration of SR95531. Due to a long application time, using higher concentrations of SR95531 is cost prohibitive. Nevertheless, we fit the data in this concentration range. Fitting the data with a single Hill equation resulted in a very shallow Hill coefficient (0.27), suggesting that it could have multiple components. Interestingly, fitting the data with a double Hill
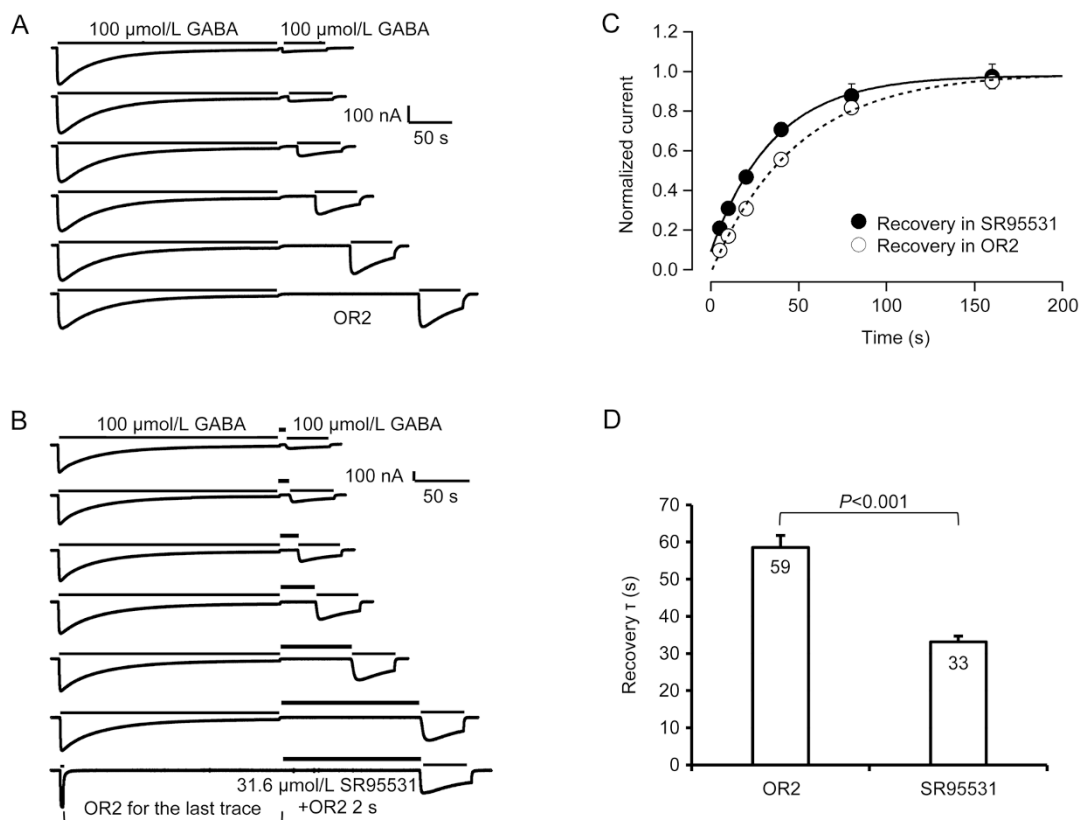

Figure 3. SR95531-facilitated recovery of desensitization in the absence of GABA. (A) Raw current traces of GABA response recovery in OR2 with different duration (*n*=5). (B) Raw current traces of GABA response recovery in SR95531 with different duration followed by a 2-s OR2 application to allow SR95531 dissociation before re-application of GABA (*n*=7). The last trace is the non-desensitization control with the initial current induced by a brief 2-s GABA application. (C) Normalized and averaged current recovery in the presence (normalized to the non-desensitization control) or absence of SR95531. The lines are fits of the data to a single exponential function. The resulting values of the time constant are plotted in D. (D) Time constants of GABA response recovery from desensitization in the presence or absence of SR95531.
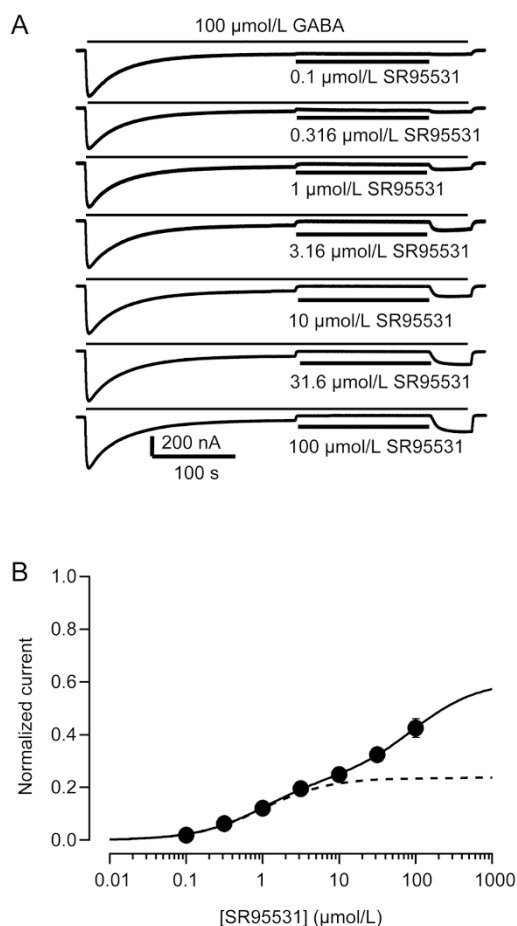
A

100 µmol/L GABA

0.1 µmol/L SR95531

0.316 µmol/L SR95531

1 µmol/L SR95531

3.16 µmol/L SR95531

10 µmol/L SR95531

31.6 µmol/L SR95531

200 nA

100 s

100 µmol/L SR95531

B

Figure 4. SR95531-facilitated recovery of desensitization is concentration dependent. (A) Raw current traces of 100 µmol/L GABA-induced desensitization recovery induced by co-application of SR95531 with increasing concentrations of SR95531. (B) SR95531 concentration dependence of the normalized and averaged current recovery (*n*=5). The continuous line is the least-squares fit of the averaged recovery data to a double Hill equation. Due to an unsaturated low potency component, the fitting of data from individual oocytes resulted in a relatively large variability. Nevertheless, it is clear that a low potency component existed. The resulting EC_{50} values are given in the text. The dashed line is the high potency component. Note that low potency component is not saturated for SR95531 at a concentration of 100 µmol/L.

equation resulted in a good fit with two components. The high potency component had an EC_{50} of 0.99 µmol/L and an I_{max} of 0.23, the low potency component had an EC_{50} of 92.3 µmol/L and an I_{max} of 0.37. Apparently, the first component saturated at the 100 µmol/L concentration of SR95531. However, the second component at 100 µmol/L was approximately at its EC_{50}. Thus, fitting for the second component was less accurate. Given that the slow dissociation of SR95531 from the receptor can reduce the maximal recovery (Figure 3), a 60% recovery (sum of the two components) is a close approximation.

Inhibition of steady-state current by SR95531 also exhibited two potency components, similar to those for desensitization recovery

The concentration-response relation of the SR95531-induced recovery of the receptor from desensitization (discussed above) revealed two potency components. To obtain further insights into the two potency components, we first performed concentration-dependent inhibition of GABA-induced peak current and steady-state current. Figure 5 shows that with the
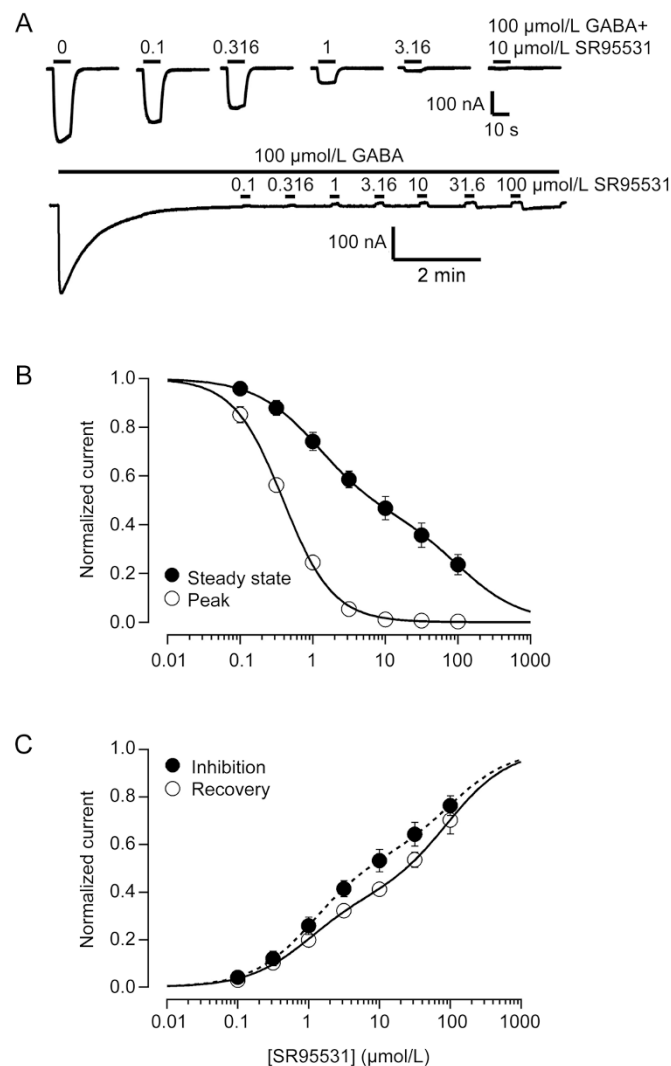

Figure 5. The potency of SR95531 in inhibiting peak current and steady-state current. (A) Concentration-dependent inhibition of 100 µmol/L GABA-induced peak current (upper) or steady-state current (lower) by SR95531. (B) Normalized and averaged peak current (*n*=6) or steady-state current (*n*=5) inhibited by SR95531. The continuous lines are a least-squares fit of single (for peak current) or double (for steady-state current) Hill equations to the data. The resulting IC_{50}s were 0.39 µmol/L for the peak inhibition and 1.2 and 103 µmol/L for the steady-state inhibition. (C) Comparison of SR95531-induced steady-state current inhibition (inverted from B) and current recovery from desensitization (from Figure 4, re-normalized to 1).

fixed concentration of GABA (100 μmol/L), co-application of SR95531 with increasing concentrations inhibited the GABA-induced peak current or steady-state current. Interestingly, SR95531 inhibition of the steady-state current could be best fitted with a double Hill equation. More interestingly, the resulting IC_{50} values of these two components were similar to the EC_{50} values observed in the SR95531-facilitated current recovery from desensitization shown in Figure 4. Figure 5C is a side-by-side comparison of SR95531 inhibition of steady-state current with the inverted and renormalized concentration response from Figure 4B. Clearly, these two potency components in both conditions were very similar.

Bicuculline also facilitated desensitization recovery of the α1β2γ2 GABA receptor

Similar to SR95531, bicuculline also exhibits an inverse agonist property. Thus, we expected to see a similar facilitation effect of bicuculline on the desensitization recovery of the GABA receptor. Indeed, Figure 6 shows that co-application of 100 μmol/L bicuculline with 100 μmol/L GABA at steady-state current level also facilitated current recovery from desensitization. However, due to an approximately 7-fold lower potency of bicuculline than SR95531 in blocking the $GABA_A$ receptor[27], it would be more difficult to construct its complete concentration-dependent effect on desensitization at a reasonable cost. Nevertheless, Figure 6 directly shows that bicuculline can also facilitate $GABA_A$ receptor recovery from desensitization.

Discussion

Indirect evidence suggests that the competitive antagonist SR95531 may also antagonize GABA-induced desensitization and facilitate recovery of the receptor from desensitization. However, direct experimental evidence is lacking. In this study, we provided three lines of evidence to support the hypothesis that SR95531 facilitates receptor recovery from desensitization. First, application of SR95531 during deactivation increased the rate of the $GABA_A$ receptor recovery from desensitization. Second, SR95531 co-application with GABA during the steady-state GABA-induced current caused rebound of the GABA-induced current after removal of SR95531, suggesting that SR95531 facilitates the recovery of the receptor from desensitization. The SR95531-facilitated recovery from desensitization was time dependent. Third, the facilitated desensitization recovery was also SR95531 concentration dependent, with a high potency component and a low potency component. Interestingly, these two potency components were very similar to the potency components of the steady-state current inhibition by SR95531. The high potency component is consistent with SR95531 binding to the re-sensitized receptors and preventing them from reentry into the desensitized state. The low potency component is consistent with the desensitized receptor having a relatively low affinity for its competitive antagonist, and that binding of a competitive antagonist to the desensitized receptor can facilitate receptor recovery from desensitization. In addition, we have also shown that bicuculline can facilitate recovery of the
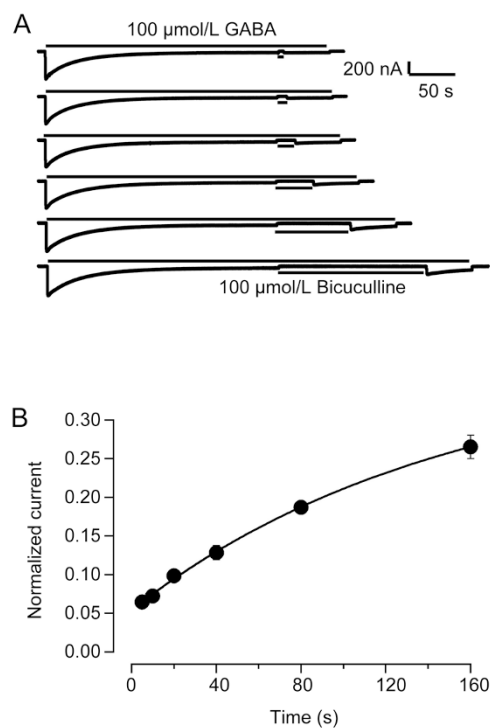

Figure 6. Bicuculline facilitated desensitization recovery of the α1β2γ2 GABA receptor. (A) Raw traces of 100 μmol/L GABA-induced current and co-application of 100 μmol/L bicuculline with varied length of duration induced recovery of desensitization of the wild-type α1β2γ2 GABA receptor. (B) Normalized (to initial peak current) and averaged current rebound after termination of bicuculline co-application (n=5). The line is the least-squares fit of the data to a single exponential function.

receptor from desensitization.

It is known that the affinity of a ligand-gated ion channel to its agonist is state dependent. The resting state has the lowest affinity, the open state has higher affinity, and the desensitized state has the highest affinity[15]. Our results also suggest that the state-dependent affinity changes of the receptor to its competitive antagonist are opposite to the affinity changes for its agonist, with high affinity in the resting state and low affinity in the desensitized state. This concept is based on the comparisons of IC_{50} values of the two potency components for blocking the 100 μmol/L GABA-induced steady-state current and the EC_{50} values of the two potency components in SR95531-facilitated recovery.

For a better clarification of our results, we performed kinetic simulations with two models: a linear model (Scheme I) with SR95531 binding only to the receptor at the resting states and a cyclic model (Scheme II) with high-affinity SR95531 bindings to the resting states and low affinity bindings to the desensitized states. In the cyclic model, the SR95531 binding to the desensitized state also facilitated the recovery of the desensitized state to the resting state (switching from low affinity to high affinity for SR95531). As shown in Figure 7, both linear and cyclic models could reproduce the current rebound as we observed. However, for SR95531 inhibition of the steady-state
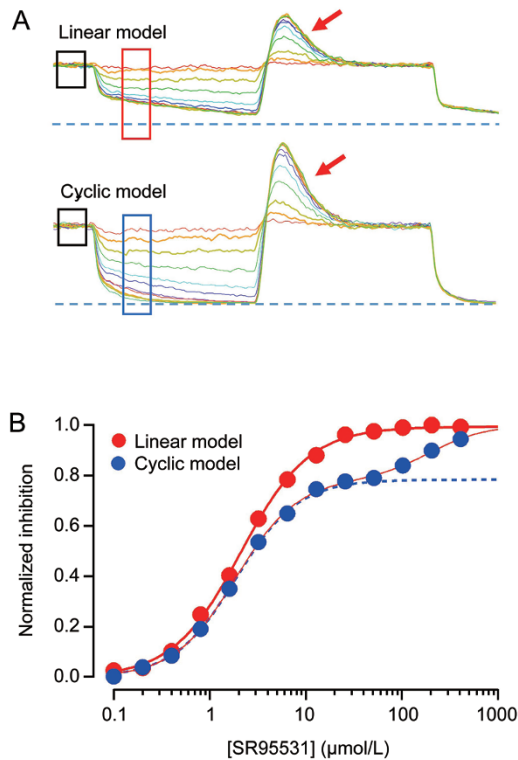
Figure 7. Simulations of the concentration-dependent inhibition of the GABA-induced steady-state current by SR95531 and current rebound upon removal of SR95531 (with 40000 channels, 100 μmol/L GABA and varied SR95531 concentrations). (A) Upper current traces were simulated with the linear model from Scheme I, with the initial GABA-induced peak current omitted. Due to current fluctuation, the average current in the black box was used as the steady-state current level and the average current in the red box was used as current inhibition level. Note that although the extent of inhibition increased over time (waiting for recovery from desensitization), the concentration-dependent change in the antagonist potency remained similar. The lower current traces were simulated with the cyclic model from Scheme II, with the initial GABA-induced peak current omitted. Similar average currents were used to calculate the concentration dependency. Note that the major difference of this simulation from that with the linear model was that higher concentrations can change the time course of current block with a low-potency component. However, if the simulation duration is sufficiently long, when nearly all the receptors recover from desensitization, the two models would be similar. Arrows indicate the rebound currents in both model simulations. (B) Concentration-dependent inhibition from the measurements in A with non-linear fits of a single Hill equation for the results from the linear model and a double Hill equation for the results from the cyclic model.

current, the linear model could not reproduce the low-potency component, whereas the cyclic model could reproduce both components. Thus, the simulation results support our conclusion that SR95531 facilitates the receptor recovery from desensitization and prevents reentry into the desensitized state after recovery. The simulation also suggests that a stable SR95531-bound state is a non-desensitized state. It is interesting that the non-competitive antagonist picrotoxin-bound state of the

GABA$_A$ receptor is also a non-desensitized state[32].

The structural basis of the agonist-induced affinity changes in the GABA$_A$ receptor is suggested by a functional test with the rate of cysteine accessibility: narrowing the orthosteric binding pocket upon channel activation[33]. The increase in GABA-binding affinity upon channel opening of the ρ1 GABA receptor is shown by single oocyte binding and a functional test[22]. Studies of the crystal structure of the ACh binding protein (AChBP; a soluble protein homologous to the N-terminal domain of a pentameric ligand-gated ion channel), co-crystallized with agonists or antagonists reveal that an agonist can induce binding loop C capping to reduce the binding pocket. However, competitive antagonists induce either no movement or uncapping of loop C to further open the binding pocket compared to the apo state[34].

More recent structural studies of the glycine receptor bound with its competitive antagonist strychnine confirmed the antagonist-induced loop C uncapping in the receptors with the channel domain[35, 36]. These studies also revealed a more complex structural rearrangement around the orthosteric binding site (Supplementary Figure 2A), including loop B and loop F moving toward the binding pocket (Supplementary Figure S2B). In contrast, AChBP crystallized with an agonist (epibatidine) does not reveal any significant movement in loop B or loop F even when compared to that with a peptide antagonist-bound state (Supplementary Figure S2C). Thus, agonist-induced loop C capping and loop B and F moving toward the binding pocket would result in narrowing of the binding pocket. These concepts can explain why the open and desensitized states have a higher agonist affinity. SR95531 and bicuculline have larger sizes than GABA. Narrowing of the orthosteric binding pocket in the desensitized states would impede the access of these competitive antagonists to the binding pocket, reduce their binding on-rate, and decrease their binding affinity. In addition, our results are also consistent with antagonist binding to the desensitized state driving the receptor back to non-desensitized states. In contrast, in the resting "apo" state, the binding sites of the receptor have larger openings, so it would be much easier for these larger competitive antagonist molecules to enter into the binding pocket. That is, for the competitive antagonists, the receptor has higher affinity in the resting state than in the open state or desensitized state. Perhaps that is why binding of a competitive antagonist to its receptor would drive the receptor out of a desensitized state toward a stable resting state. In other words, in equilibrium, the competitive antagonist bound state is a non-desensitized state. These conclusions are also supported by our simulations (discussed above).

Can differential residues in the binding pocket interacting with the agonist or the antagonist contribute to their differential effects on desensitization in addition to the size of the ligand? For SR95531 and GABA, cysteine scanning mutagenesis studies would provide clues. In Supplementary Figure S3, we plotted the impact of cysteine mutations on the fold changes of K_i of SR95531 and EC$_{50}$ of GABA previously reported[33, 37–41]. While most cysteine mutants showed higher-

fold changes in GABA EC_{50} than the fold changes of SR95531 K_i, one mutation, F64C (black-filled circle), exhibited higher impact on the K_i of SR95531. This is a binding residue in the loop D of the α1 subunit. The homologous residue (Trp55) in nAChRα7 has been identified as a residue that can significantly influence channel gating, the mutation of which can dramatically influence desensitization kinetics[42]. Thus, it is possible that GABA and SR95531 interact with this residue differently. Specifically, GABA interaction with this residue would induce a conformational change to facilitate desensitization, whereas SR95531 interaction likely induces an opposite conformational change to facilitate the recovery from desensitization. There are 4 residues (gray-filled cycles), the cysteine mutations of which resulted in more than a 1000-fold increase in the GABA EC_{50}. These are clearly important binding residues. In contrast, the mutational influence of these 4 residues on SR95531 K_i is much smaller (10–100 fold). The higher impact of the mutations of these residues on the agonist EC_{50} suggests that they are important in channel gating. These residues are E155 in loop B and T202, G203 and Y205 in loop C. In fact, β2Glu155 has been suggested as a trigger of channel gating. Interaction of these "gating" residues with GABA would induce conformational changes, such as loop C capping, to open and then desensitize the receptor. In contrast, a competitive antagonist could induce the opposite conformational changes, such as loop C uncapping to facilitate desensitization recovery.

In the $GABA_A$ receptor, we previously showed that in intact living oocytes, the dissociation of ^3H-GABA from the desensitized state has a time constant of 30 s, and the recovery of the receptor from desensitization is approximately 4-fold slower than the GABA dissociation[24]. Thus, after agonist dissociation, the receptor still remains in a desensitized state for a relatively long time. This would allow the competitive antagonists to complete with GABA for the same binding site in the desensitized state.

In addition, in the steady-state desensitization level, the GABA-induced current is not completely desensitized, even at very high GABA concentrations. Approximately 5% of the $GABA_A$ receptors remain non-desensitized at equilibrium even with continuous presence of 10 000 μmol/L GABA[24]. This equilibrium state had already saturated at 300 μmol/L GABA. Figure 8 shows that, in fact, continuous application of 100 μmol/L GABA also reached a steady-state level that cannot be further desensitized by 1000 μmol/L GABA. Thus, at the steady-state current level during GABA application, receptors reach the equilibrium between entering the open state and desensitized state and recovering from desensitization. That is, at steady-state desensitization equilibrium, the competitive antagonists compete with GABA not only for desensitized receptors but also for a small fraction of receptors in the non-desensitized state. This can explain why we observed two potency components in the SR95531 inhibition of steady-state current, as well as in SR95531 facilitation of desensitization recovery. The high potency component is consistent with the SR95531 binding to the re-sensitized receptors, preventing
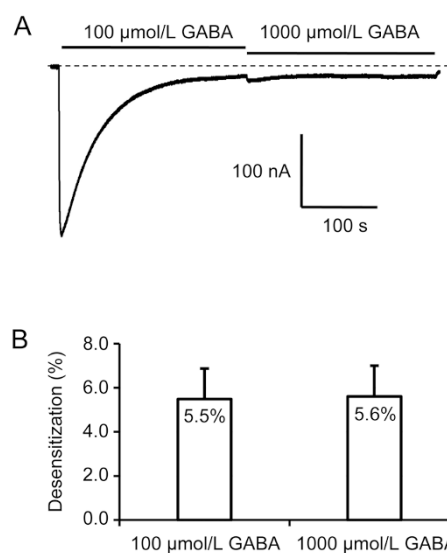

Figure 8. 100 and 1000 μmol/L GABA-induced desensitization of the α1β2γ2 GABA receptor. (A) Raw traces of current induced by 100 and 1000 μmol/L GABA. (B) Normalized (to peak current) and averaged steady-state desensitized current level at two GABA concentrations (*n*=10).

these receptors from re-entering into the desensitized state. The low potency component would reflect the binding to the low-affinity desensitized state for the antagonist. Because we also observed a similar low-potency component in current inhibition for steady-state current, the low affinity state(s) may represent a combination of open and desensitized states with mutual transitions. For example, desensitization can prolong the current activation response[19]. In addition, even in the activated state, a receptor can still isomerize between open and flipped high-affinity states[43]. It is unknown whether a competitive antagonist has similar low affinity to the flipped state and desensitized state. However, the flipped state model suggests that the receptor must return to a non-flipped state before the agonist can dissociate. In contrast, the cyclic desensitization model has been confirmed by the experimental observation that the agonist can dissociate from the desensitized state. In addition, our data also show the SR95531-facilitated recovery of the receptor from a desensitized state in the absence GABA. Thus, it is more likely that the low-potency component represents the binding of SR95531 to the desensitized state, and binding of the competitive antagonist to the receptor would induce conformational changes to reverse the desensitization, as predicted in our simulation (Figure 7) using Scheme II.

Can binding of a noncompetitive antagonist induce further conformational change of the receptor from the apo state? This would depend on the actual size of each competitive antagonist. For example, homology modeling, agonist/antagonist docking, and molecular dynamic simulation of the glycine receptor reveal that binding of the competitive antagonist strychnine induces conformational changes (uncapping) in loop C and in the transmembrane domain[44]. Recent struc-

tural studies of glycine receptors with strychnine binding further confirmed that the competitive antagonist can induce further structural changes beyond the apo (resting) state in the opposite direction of the agonist-induced channel opening and desensitization[35, 36]. In addition to the structural changes in the extracellular binding domain, when compared to the apo state of the glutamate gated chloride channel[8], the competitive antagonist induces further contraction of the coupling region (including the M2–M3 linker) and narrowing of the extracellular side of the channel domain and expansion of the intracellular side of the channel. This is in distinct contrast to the opposite structural changes in the channel domain in a putative open state of glutamate-gated chloride channel bound with an allosteric agonist, ivermectin[45], and a putative desensitized state of the agonist benzamidine-bound homomeric GABA$_A$ receptor[46]. Thus, it is possible that SR95531 and bicuculline can induce the uncapping of loop C as well as changes in other parts (including the transmembrane domain) of the receptor and actively antagonize the GABA-induced conformational changes related to desensitization.

Bicuculline has a larger size than SR95531. It may cause a slightly larger uncapping of loop C than SR95531, resulting in a larger "inverse agonist" effect. Indeed, with the spontaneously opening mutant GABA$_A$ receptor, bicuculline blocks 41% of the spontaneous current, whereas SR95531 only blocks 13% of the spontaneous current[27]. With the overexpressed wild-type GABA$_A$ receptor with spontaneous openings, the maximal antagonism for spontaneously opening current was higher for bicuculline than that for SR95531 (Figure 9). Note that the spontaneously opening current of the overexpressed α1β2γ2 receptor was not due to the homomeric β2 receptors because they were not sensitive to zinc inhibition as seen in the β2 homomers (Figure 9). We can speculate that bicuculline may have a larger inverse agonist effect on desensitization. However, due to its lower affinity than SR95531, it is impractical to determine its efficacy (and EC$_{50}$) for the "inverse agonist" effect for the desensitized state.

In summary, we have provided experimental evidence to support the hypothesis that binding of the GABA$_A$ receptor competitive antagonists, SR95531 and bicuculline, can facilitate the recovery of the receptor from desensitization or prevent its re-entry into the desensitized state. It would be interesting to determine whether a similar phenomenon exists in other members of the pentameric ligand-gated ion channel superfamily. In fact, we have observed the current rebound in the ρ1 GABA$_A$ receptor during agonist application co-treated with a competitive antagonist, 3-aminopropylphosphonic acid (Supplementary Figure S4), suggesting that this is a potentially general phenomenon for all members of this receptor superfamily.
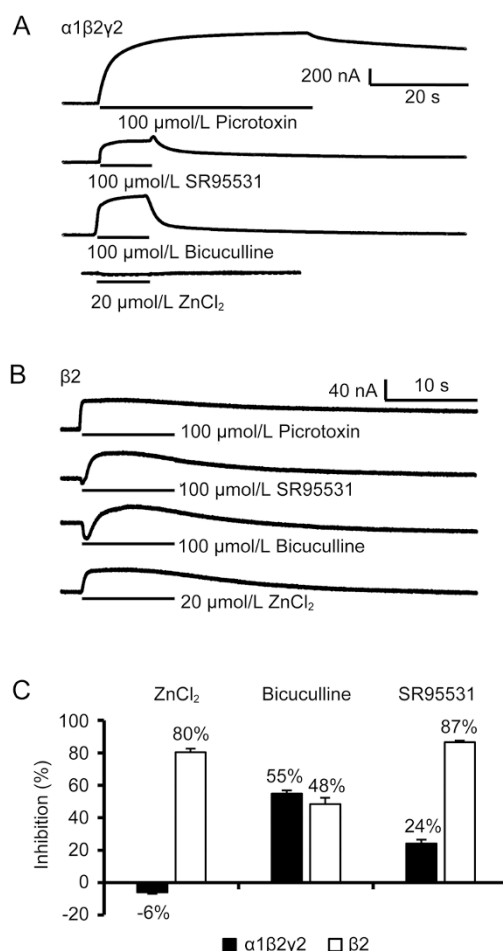
Acknowledgements

Figure 9. Comparison of the efficacy of bicuculline and SR95531 as inverse agonists in blocking the spontaneous current of the overexpressed wild type α1β2γ2 GABA receptor. (A) Raw traces of current show inhibition of the spontaneous current by a saturation concentration (to the wild-type α1β2γ2 GABA receptor) of SR95531, bicuculline, and picrotoxin. Note that it was not sensitive to 20 μmol/L ZnCl$_2$ inhibition. (B) Raw current traces of the homomeric β2 GABA receptor control. Its spontaneous current was sensitive to 20 mol/L ZnCl$_2$ inhibition. The spontaneous current was also inhibited by the other antagonists. (C) Normalized (to 100 μmol/L picrotoxin inhibitable current) and averaged inhibition of bicuculline and SR95531 for the α1β2γ2 heteromeric GABA$_A$ receptor (*n*=9) or β2 homomeric GABA$_A$ receptor.

Author contribution

Abbreviations

GABA, γ-aminobutyric acid; OR2, oocyte Ringer's solution 2; HEPES, 4-(2-hydroxyethyl)piperazine-1-ethanesulfonic acid; AChBP, ACh binding protein; 3-APA, 3-aminopropylphos-

phonic acid.

Supplementary information

Supplementary Figures are available at the Acta Pharmacologica Sinica's website.

References

1 Lester H, Dibas M, Dahan D, Leite J, Dougherty D. Cys-loop receptors: new twists and turns. Trends Neurosci 2004; 27: 329–36.

2 Sine S, Engel A. Recent advances in Cys-loop receptor structure and function. Nature 2006; 440: 448–55.

3 Albuquerque E, Pereira E, Alkondon M, Rogers S. Mammalian nicotinic acetylcholine receptors: from structure to function. Physiol Rev 2009; 89: 73–120.

4 Lummis S. 5-HT$_3$ receptors. J Biol Chem 2012; 287: 40239–45.

5 Olsen R, Sieghart W. GABA$_A$ receptors: subtypes provide diversity of function and pharmacology. Neuropharmacology 2009; 56: 273–84.

6 Lynch J. Native glycine receptor subtypes and their physiological roles. Neuropharmacology 2009; 56: 303–9.

7 Davies P, Wang W, Hales T, Kirkness E. A novel class of ligand-gated ion channel is activated by Zn^{2+}. J Biol Chem 2003; 278: 712–7.

8 Althoff T, Hibbs R, Banerjee S, Gouaux E. X-ray structures of GluCl in apo states reveal a gating mechanism of Cys-loop receptors. Nature 2014; 512: 333–7.

9 Beg A, Jorgensen E. EXP-1 is an excitatory GABA-gated cation channel. Nat Neurosci 2003; 6: 1145–52.

10 Zheng Y, Hirschberg B, Yuan J, Wang A, Hunt D, Ludmerer S, *et al.* Identification of two novel *Drosophila melanogaster* histamine-gated chloride channel subunits expressed in the eye. J Biol Chem 2002; 277: 2000–5.

11 Ranganathan R, Cannon S, Horvitz H. MOD-1 is a serotonin-gated chloride channel that modulates locomotory behaviour in *C elegans*. Nature 2000; 408: 470–5.

12 Bocquet N, Nury H, Baaden M, Poupon C, Changeux J, Delarue M, *et al.* X-ray structure of a pentameric ligand-gated ion channel in an apparently open conformation. Nature 2009; 457: 111–4.

13 Hilf R, Dutzler R. Structure of a potentially open state of a proton-activated pentameric ligand-gated ion channel. Nature 2009; 457: 115–9.

14 Chang Y, Wu W, Zhang J, Huang Y. Allosteric activation mechanism of the cys-loop receptors. Acta Pharmacol Sin 2009; 30: 663–72.

15 Colquhoun D. Binding, gating, affinity, and efficacy: the interpretation of structure-activity relationships for agonists and of the effects of mutating receptors. Br J Pharmacol 1998; 125: 923–48.

16 del Castillo J, Katz B. Interaction at end-plate receptors between different choline derivatives. Proc R Soc Lond B Biol Sci 1957; 146: 369–81.

17 Katz B, Thesleff S. A study of the desensitization produced by acetylcholine at the motor end-plate. J Physiol 1957; 138: 63–80.

18 Giniatullin R, Nistri A, Yakel J. Desensitization of nicotinic ACh receptors: shaping cholinergic signaling. Trends Neurosci 2005; 28: 371–8.

19 Jones M, Westbrook G. Desensitized states prolong GABA$_A$ channel responses to brief agonist pulses. Neuron 1995; 15: 181–91.

20 Chen Y, Reilly K, Chang Y. Evolutionarily conserved allosteric network in the cys-loop family of ligand-gated ion channels revealed by statistical covariance analyses. J Biol Chem 2006; 281: 18184–92.

21 Changeux J, Edelstein S. Allosteric receptors after 30 years. Neuron 1998; 21: 959–80.

22 Chang Y, Weiss D. Channel opening locks agonist onto the GABA$_C$ receptor. Nat Neurosci 1999; 2: 219–25.

23 Chang Y, Weiss D. Site-specific fluorescence reveals distinct structural changes with GABA receptor activation and antagonism. Nat Neurosci 2002; 5: 1163–8.

24 Chang Y, Ghansah E, Chen Y, Ye J, Weiss D. Desensitization mechanism of GABA receptor revealed by single oocyte binding and receptor function. J Neurosci 2002; 22: 7982–90.

25 Scheller M, Forman S. Coupled and uncoupled gating and desensitization effects by pore domain mutations in GABA$_A$ receptors. J Neurosci 2002; 22: 8411–21.

26 Bartrup J, Newberry N. Electrophysiological consequences of ligand binding to the desensitized 5-HT3 receptor in mammalian NG108-15 cells. J Physiol 1996; 490: 679–90.

27 Chang Y, Weiss D. Allosteric activation mechanism of the α1β2γ2 γ-aminobutyric acid type A receptor revealed by mutation of the conserved M2 leucine. Biophys J 1999; 77: 2542–51.

28 Ueno S, Bracamontes J, Zorumski C, Weiss D, Steinbach J. Bicuculline and gabazine are allosteric inhibitors of channel opening of the GABA$_A$ receptor. J Neurosci 1997; 17: 625–34.

29 Lüddens H, Korpi E. GABA antagonists differentiate between recombinant GABA$_A$/benzodiazepine receptor subtypes. J Neurosci 1995; 15: 6957–62.

30 Nicolai C, Sachs F. Solving ion channel kinetics with the QuB software. Biophys Rev Lett 2013; 8: 1–21.

31 Amin J, Weiss DS. GABA$_A$ receptor needs two homologous domains of the b subunit for activation by GABA, but not by pentobarbital. Nature 1993; 366: 565–9.

32 Gielen M, Thomas P, Smart T. The desensitization gate of inhibitory Cys-loop receptors. Nat Commun 2015; 6: 6829.

33 Wagner D, Czajkowski C. Structure and dynamics of the GABA binding pocket: a narrowing cleft that constricts during activation. J Neurosci 2001; 21: 67–74.

34 Hansen S, Sulzenbacher G, Huxford T, Marchot P, Taylor P, Bourne Y. Structures of Aplysia AChBP complexes with nicotinic agonists and antagonists reveal distinctive binding interfaces and conformations. EMBO J 2005; 24: 3635–46.

35 Huang X, Chen H, Michelsen K, Schneider S, Shaffer P. Crystal structure of human glycine receptor-α3 bound to antagonist strychnine. Nature 2015; 526: 277–80.

36 Du J, Lu W, Wu S, Cheng Y, Gouaux E. Glycine receptor mechanism elucidated by electron cryo-microscopy. Nature 2015; 526: 224–9.

37 Newell J, Czajkowski C. The GABA$_A$ receptor α1 subunit Pro^{174}–Asp^{191} segment is involved in GABA binding and channel gating. J Biol Chem 2003; 278: 13166–72.

38 Boileau A, Glen Newell J, Czajkowski C. GABA$_A$ receptor β2 Tyr97 and Leu99 line the GABA-binding site: Insights into mechanisms of agonist and antagonist actions. J Biol Chem 2002; 277: 2931–7.

39 Newell J, McDevitt R, Czajkowski C. Mutation of glutamate 155 of the GABA$_A$ receptor β2 subunit produces a spontaneously open channel: a trigger for channel activation. J Neurosci 2004; 24: 11226–35.

40 Holden J, Czajkowski C. Different residues in the GABA$_A$ receptor α1T60-α1K70 region mediate GABA and SR-95531 actions. J Biol Chem 2002; 277: 18785–92.

41 Kloda J, Czajkowski C. Agonist-, antagonist-, and benzodiazepine-Induced structural changes in the α1Met113-Leu132 region of the GABA$_A$ receptor. Mol Pharmacol 2007; 71: 483–93.

42 Gay E, Giniatullin R, Skorinkin A, Yakel J. Aromatic residues at position 55 of rat α7 nicotinic acetylcholine receptors are critical for maintaining rapid desensitization. J Physiol 2008; 586: 1105–15.

43 Lape R, Colquhoun D, Sivilotti L. On the nature of partial agonism in the nicotinic receptor superfamily. Nature 2008; 454: 722–7.

44 Yu R, Hurdiss E, Greiner T, Lape R, Sivilotti L, Biggin P. Agonist and antagonist binding in human glycine receptors. Biochemistry 2014; 53: 6041–51.

45 Hibbs R, Gouaux E. Principles of activation and permeation in an anion-selective Cys-loop receptor. Nature 2011; 474: 54–60.

46 Millar P, Aricescu A. Crystal structure of a human GABA$_A$ receptor. Nature 2014; 512: 270–5.